IET Generation, Transmission & Distribution

Research Article

IET Journals
The Institution of Engineering and Technology

Decentralised robust T-S fuzzy controller for a parallel islanded AC microgrid

ISSN 1751-8687
Received on 31st October 2017
Revised 5th August 2018
Accepted on 18th December 2018
E-First on 4th April 2019
doi: 10.1049/iet-gtd.2018.5757
www.ietdl.org

Teimour Hosseinalizadeh[1], *Hamed Kebriaei*[1,2] ✉, *Farzad Rajaei Salmasi*[1]

[1]*School of ECE, College of Engineering, University of Tehran, Tehran, Iran*
[2]*School of Computer Science, Institute for Research in Fundamental Sciences (IPM), Tehran, Iran*
✉ *E-mail: kebriaei@ut.ac.ir*

Abstract: This study proposes a decentralised robust fuzzy control strategy for islanded operation of an AC microgrid with voltage source inverters. The objective is to design a robust controller for regulating the load voltage and sharing power among distributed generators (DGs) in the presence of uncertainties in the system and non-linear loads. The AC microgrid consists of parallel DGs connected to a main AC bus. A Takagi-Sugeno fuzzy approach is developed in this article to achieve stability and desired performance in dealing with non-linearities in the islanded microgrid and H_∞ criterion is used to obtain a robust control strategy in presence of uncertainties raised by unmodelled and high frequency dynamics. Therefore, a non-convex condition in H_∞ optimisation problem is converted to a convex linear matrix inequality (LMI) condition and is solved by MATLAB LMI toolbox. In order to develop a decentralized system, *P–f* and *Q–V* droop controllers are used to specify set-points for local inverter controllers in each DG. The effectiveness of the proposed control strategy in presence of constant power load and DG accidental outage is validated by the simulation of a microgrid test system in MATLAB SimPowerSystems toolbox. Comparison with cascaded proportional integral controller shows advantages of robust T-S controller.

1 Introduction

Today a considerable share of the electrical energy needed for various consumptions is provided by renewable energy sources such as solar and wind powers. Microgrids, as an emerging technology in power systems, integrate small- and medium-sized DGs and connect them to the main electricity grid. A microgrid can operate in the islanded mode when it is disconnected from the main grid because of faults or pre-planned events. However, islanded operation of microgrids imposes unsatisfactory dynamical responses such as voltage and frequency fluctuations or even instabilities [1, 2]. Therefore, appropriate controlling of the microgrids can increase the power quality and reliability of electricity provided to the loads.

Microgrid control strategies can be divided into two main categories: (i) centralised (non-droop based) and (ii) decentralised (droop based). The centralised controller needs communication among DGs and uses a high share of bandwidth to control the microgrid. However, droop-based controller does not need high bandwidth communications, because it mainly uses DGs' characteristics to decide on main variables in the microgrid. Moreover, centralised controller may cause failure of the whole microgrid if one of the units fails down, nevertheless, decentralised strategies provide more reliability in the case of DG failure [3]. Although droop-based control can cause voltage and frequency deviations, hierarchical strategies including primary, secondary, and tertiary can compensate such deviations [4].

In recent years, numerous control strategies to control DG-based microgrids have been proposed. Linear robust controller with high reliability has been widely used in the literature. In [5], authors have proposed a power management system and a robust control strategy for an autonomous microgrid with pre-defined load dynamics. However, no discussion has been made about load sharing among DGs using decentralised controller and also they assumed a GPS-based common time-reference signal is available to DGs for controlling frequency of the system. However, the system becomes vulnerable due to any possible faults in this signal. In [6], a master–slave 2DOF controller is utilised to control microgrid using communication among DGs. However, the master–slave method cannot be effective in the case of communication faults and delays. Moreover, the performance of such controller has not been evaluated for highly non-linear load such as constant power loads (CPLs). Karimi *et al*. [7] have proposed a control strategy for an autonomous four-wired microgrid. However, since the load model is specified to be used for designing controller, if the load structure changes, the controller should be redesigned. Furthermore, no discussion is made about power sharing among DGs. In [8], a fully centralised controller for power management in an AC microgrid has been proposed. As it was mentioned before, the system vulnerability is increased in centralised structure due to the faults in communication system.

Use of non-linear controller with large region of attraction can provide better performance in a wide range of operation points [9–13]. In [10], robust feedback linearisation is utilised for controlling an islanded AC microgrid with parametric uncertainty by canceling the intrinsic non-linearities within the defined structure. However, this method imposes a restrictive assumption for uncertain dynamics and also it cannot be used in case of unmatched uncertainty in input channel. Cucuzzella *et al*. [11] first proposed second-order sliding mode controller for a master–slave microgrid system and after that, to alleviate chattering problem designed a higher order sliding mode controller. Main restrictive assumption in this paper is considering linear load model in controller design procedure which makes controller performance unsatisfactory in case of non-linear load dynamics. In [12], backstepping controller is applied to an inverter in both islanded and grid connected modes. In this approach, unbounded amplitude pulses and chattering phenomena may occur because of variables with the second derivative and also non-smooth function in control law. Mahmud *et al*. [13] used robust feedback linearisation theory for controlling 3-phase grid connected inverter, but the main drawback of the approach is that it is not extendable to other AC microgrid topologies.

Fuzzy logic has been widely used in AC, DC and hybrid microgrid systems for energy management, voltage and frequency regulation purposes [14–20]. A neuro-fuzzy controller based on data analytics is suggested in [15] to guarantee stable operation of AC microgrid in both grid connected and isolated modes. Sefa *et al*. [16] has designed proportional integral (PI) controlled grid interactive inverter where parameters of PI are tuned by fuzzy logic

controllers. Although design procedure is intuitive in Mamdani-type fuzzy system, but expert knowledge is needed for designing fuzzy rules and moreover, stability of the system is not guaranteed theoretically in both of the papers. In [17] fuzzy logic controller is applied to a microgrid with a single voltage source inverter (VSI) for controlling load voltage by ignoring the load variability and uncertainty. However, the defined microgrid structure is relatively simple and also due to Mamdani-type fuzzy controller designing method, stability of the system is not explored. Bevrani *et al*. [18] have proposed a combination of the fuzzy logic and the particle swarm optimisation techniques for optimal tuning PI controller in AC microgrid. However, considering power resources as a linear time invariant system limits the approach to be applicable for AC microgrids. In [20], a DC distribution voltage control for DC/DC converters which combines a gain-scheduling procedure with fuzzy control is proposed. The main benefit of the proposed control is where the load model is unknown or is mathematically complex. However, the fuzzy membership functions are regulated by trial and error method. It is inferred from the above discussion that, designing a decentralised non-linear robust controller with smooth feasible signal, applicable in a wide range of load dynamics, is important in AC microgrid. Therefore, the main purpose of this paper is to design a controller with such capabilities.

This paper presents a fuzzy decentralised robust control strategy for an islanded AC microgrid, comprising several DG units with voltage source inverters. First, the mathematical model of a three-phase voltage source inverter with output LC filter and general connected load (linear or non-linear) is presented. The corresponding non-linear state-space model for the inverter with LC filter is obtained using instantaneous power balance between the inverter output terminal and the load side. Then, a Takagi–Sugeno (T-S) fuzzy interference system is designed to model the above system. In fuzzy linearised model, a lumped uncertainty (Δ) has been considered as a finite energy uncertainty, representing the unmodelled and high frequency dynamics. Therefore, L_2 norm in controller design is needed to guarantee the robustness against it. This problem is solvable in the context of H_∞ method without unnecessary conservativeness. Other robust methods such as L_1 and sliding mode controller impose excessive assumptions which are neither realistic nor applicable in the microgrid systems. In order to design T-S H_∞ controller, a non-convex optimisation problem to achieve L_2 gain performance and robust stability criteria are formulated. Then, the non-convex optimisation problem is converted to a convex linear matrix inequality (LMI). The LMI conditions are solved by MATLAB LMI toolbox in finite time which is another advantage of the proposed H_∞ approach. Also, P–f and Q–V droop controllers are utilised to share desired active and reactive power among DGs based on their power capacities. The performance of the proposed control strategy is verified by performing three case studies simulated in the MATLAB/SimPowerSystems toolbox. The results show that the proposed T-S robust controller is effectively capable to regulate the point of common coupling (PCC) voltage and frequency for linear and non-linear loads and also in case of an accidental outage of a DG. Moreover, comparison with the conventional cascaded PI controller illustrates the advantages of T-S robust controller for the studied microgrid. The contributions of the paper could be summarised as follows: (see (1))

- Deriving T-S fuzzy model of an AC microgrid using non-linear sector method
- Designing a decentralised non-linear robust T-S-based controller through convex optimisation and LMI formulation for the VSIs in the AC microgrid
- Providing sufficient conditions for the robust performance of the microgrid system, while power sharing among DGs are achieved through droop controllers
- Verifying the proposed controller performance in case of highly non-linear loads and accidental outage of DGs, and
- Comparing controller performance with the conventional cascaded PI controller

The paper is organised as follows: Section 2 describes the system under study. In Section 3, fuzzy T-S model of AC microgrid is derived. Section 4 provides T-S H_∞ robust controller design for the system under study. In Section 5, simulation analysis and comparison with the cascaded PI controller are investigated. Section 6 draws the conclusion of the paper.

2 AC microgrid modeling

2.1 DG modeling

In an islanded AC microgrid, there is a main AC bus which is connected to the distributed resources and/or energy storage systems through power converter/inverters and appropriate filters. The AC bus feeds the local loads. In order to derive a mathematical model for such a system, first we consider a simplified structure as shown in Fig. 1, in which a VSI is connected to the AC bus through an LC filter. The DC side of the converter is connected to an energy source/storage system such as photovoltaic, wind turbine, or storage device. Without loss of generality, such energy source/storage system provides almost a constant DC-bus voltage for the VSI input. Therefore, no dynamics is considered for the DC side here. Moreover, C_f and L_f are the filter parameters.

Using Kirchhoff's voltage and current laws, one can obtain the system equations as follows:

$$\begin{cases} \dfrac{\mathrm{d}i}{\mathrm{d}t} = \dfrac{1}{L_\mathrm{f}} v_i - \dfrac{1}{L_\mathrm{f}} v \\ \dfrac{\mathrm{d}v}{\mathrm{d}t} = \dfrac{1}{C_\mathrm{f}} i - \dfrac{1}{C_\mathrm{f}} i_l . \end{cases} \tag{2}$$

$$\begin{pmatrix} \dot{v}_d \\ \dot{v}_q \\ \dot{i}_d \\ \dot{i}_q \end{pmatrix} = \begin{pmatrix} (x_c \omega_b z_b)\left(\dfrac{1}{z_b} i_d - \left(\dfrac{s_b}{v_b^2}\right)\dfrac{p_f}{v_d^2 + v_q^2} v_d - \dfrac{(s_b/v_b^2) q_f - (\omega_\mathrm{pu}/z_b) x_{L_\mathrm{pu}} (i_d^2 + i_q^2)}{v_d^2 + v_q^2} v_q\right) \\ (x_c \omega_b z_b)\left(\dfrac{1}{z_b} i_q - \left(\dfrac{s_b}{v_b^2}\right)\dfrac{p_f}{v_d^2 + v_q^2} v_q + \dfrac{(s_b/v_b^2) q_f - (\omega_\mathrm{pu}/z_b) x_{L_\mathrm{pu}} (i_d^2 + i_q^2)}{v_d^2 + v_q^2} v_d\right) \\ (\omega_\mathrm{pu}\omega_b) i_q - \dfrac{\omega_b}{x_{L_\mathrm{pu}}} v_d \\ -(\omega_\mathrm{pu}\omega_b) i_d - \dfrac{\omega_b}{x_{L_\mathrm{pu}}} v_q \end{pmatrix} + \begin{pmatrix} 0 & 0 \\ 0 & 0 \\ \dfrac{\omega_b}{x_{L_\mathrm{pu}}} & 0 \\ 0 & \dfrac{\omega_b}{x_{L_\mathrm{pu}}} \end{pmatrix} \begin{pmatrix} v_{id} \\ v_{iq} \end{pmatrix} \tag{1}$$

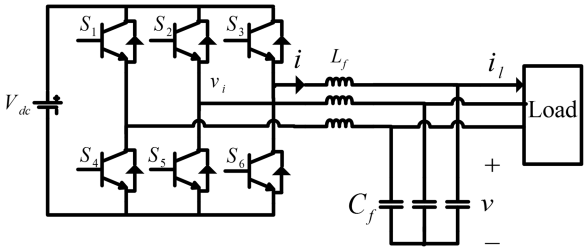

Fig. 1 *Single DG unit connected to an unknown load*

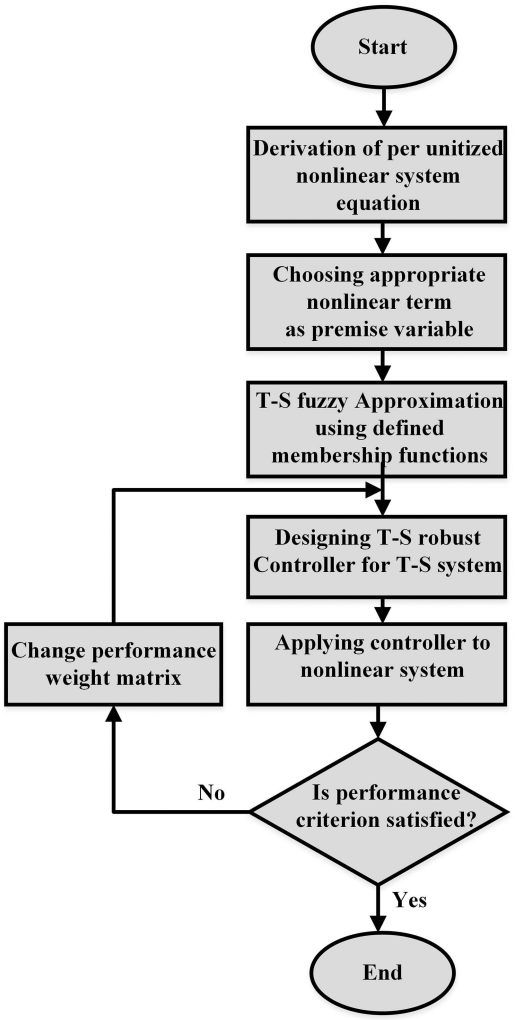

Fig. 2 *Controller design procedure used in this paper*

where v and i_l stand for the three phase load voltages and currents, respectively, v_i represents the input voltage and i is the inductor current. The above equations are transformed using Park transformation as follows:

$$\begin{pmatrix} \dot{v}_d \\ \dot{v}_q \\ \dot{i}_d \\ \dot{i}_q \end{pmatrix} = \begin{pmatrix} \omega v_d - \frac{1}{C_f} i_{lq} + \frac{1}{C_f} i_q \\ \omega v_d - \frac{1}{C_f} i_{lq} + \frac{1}{C_f} i_q \\ -\frac{1}{L_f} v_d + \omega i_d + \frac{1}{L_f} v_{id} \\ -\frac{1}{L_f} v_q - \omega i_q + \frac{1}{L_f} v_{iq} \end{pmatrix} \tag{3}$$

where (3) shows mathematical model in the dq framework. Defining p_f and q_f as instantaneous inverter output active power and reactive power, respectively, i_{ld} and i_{lq} can be represented as functions of p_f and q_f as follows [21, 22]:

$$\begin{aligned} p_f &= v_d i_{Ld} + v_q i_{Lq} \\ q_f &= v_q i_{Ld} - v_d i_{Lq} - \omega c_f |v_{dq}|^2 + \omega L_f |i_{dq}|^2 \end{aligned} \tag{4}$$

By solving (4) one can get i_{ld} and i_{lq} as

$$\begin{aligned} i_{ld} &= \frac{p_f v_d + q_f v_d}{v_d^2 + v_q^2} + \omega C_f v_d - \frac{\omega L_f (i_d^2 + i_q^2) v_q}{v_d^2 + v_q^2} \\ i_{lq} &= \frac{p_f v_q - q_f v_d}{v_d^2 + v_q^2} - \omega C_f v_d + \frac{\omega L_f (i_d^2 + i_q^2) v_d}{v_d^2 + v_q^2} \end{aligned} \tag{5}$$

Using (3) and (5) state-space model of the system can be reformulated as

$$\begin{aligned} \begin{pmatrix} \dot{v}_d \\ \dot{v}_q \\ \dot{i}_d \\ \dot{i}_q \end{pmatrix} &= \begin{pmatrix} \frac{1}{C_f}\left(i_d - \frac{p_f}{(v_d^2 + v_q^2)} v_d - \frac{q_f - \omega L_f (i_d^2 + i_q^2)}{(v_d^2 + v_q^2)} v_q\right) \\ \frac{1}{C_f}\left(i_q - \frac{p_f}{(v_d^2 + v_q^2)} v_q + \frac{q_f - \omega L_f (i_d^2 + i_q^2)}{(v_d^2 + v_q^2)} v_d\right) \\ \omega i_q - \frac{1}{L_f} v_d \\ -\omega i_d - \frac{1}{L_f} v_q \end{pmatrix} \\ &+ \begin{pmatrix} 0 & 0 \\ 0 & 0 \\ \frac{1}{L_f} & 0 \\ 0 & \frac{1}{L_f} \end{pmatrix} \begin{pmatrix} v_{id} \\ v_{iq} \end{pmatrix} \\ y &= \begin{pmatrix} v_d \\ v_q \end{pmatrix}. \end{aligned} \tag{6}$$

2.2 Design procedure

In Fig. 2, controller design procedure pursued in this paper is shown. First, the system (6) is per unitised using S_{base} and V_{base}. Then, it can be represented as (1) in this step. After that, the non-linear terms in (1) are appropriated by the fuzzy premise variables and their corresponding membership functions are defined. Next, T-S robust controller is designed for T-S fuzzy approximation of the non-linear system and at the end, controller is applied to the actual non-linear system. Details of each step are explained thoroughly in the following sections.

It should be noted that conventional droop controllers are used for power sharing between DGs in the microgrid. The voltage and frequency droop characteristics for the ith DG are as follows:

$$\begin{cases} f_i = f_n - m_i (P_i - P_i^n) \\ V_i = V_n - n_i (Q_i - Q_i^n) \end{cases} \tag{7}$$

where f_n and V_n are nominal frequency and nominal voltage magnitude, respectively, m_i and n_i are the droop coefficients which are chosen based on the active and reactive power ratings of each DGs, P_i and Q_i are the active and reactive power of each DGs measured at the DG's output terminal and then filtered by a low-pass filter (LPF) and P_i^n, Q_i^n are nominal active and reactive power for each DG, respectively. V_i and f_i are the voltage magnitude and frequency references for the primary controller (proposed robust T-S controller), respectively. The block diagram of the overall system is shown in Fig. 3 for an AC microgrid with two distributed resources. Designing an output non-linear robust controller for (1) is not a straightforward procedure. Therefore, in the next section, we aim to derive a fuzzy T-S description of the system to facilitate the design objectives.

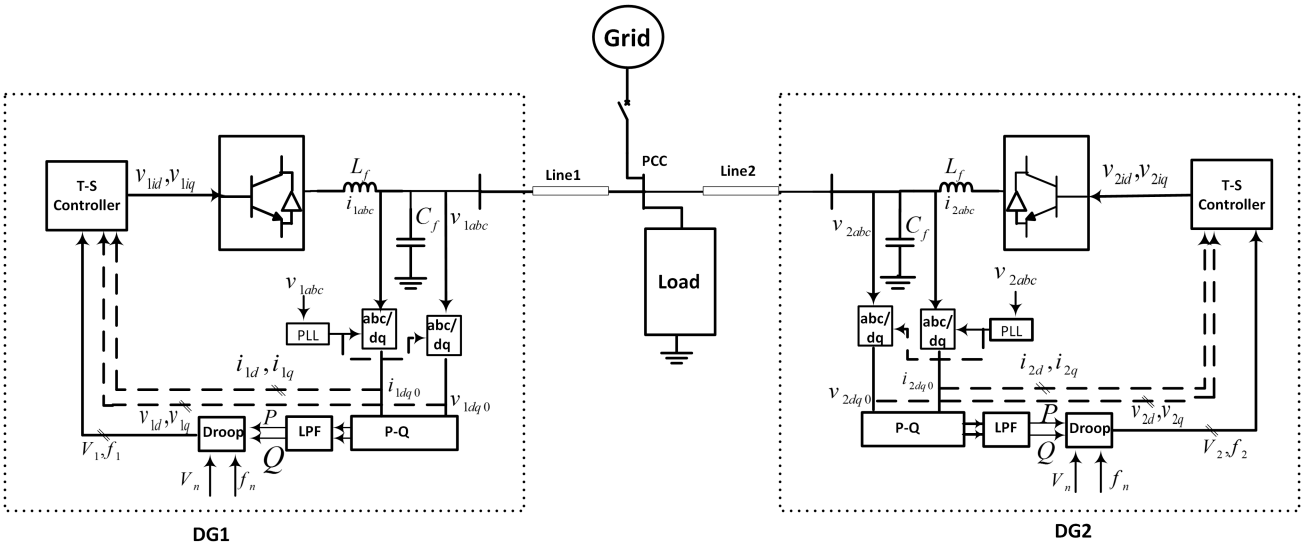

Fig. 3 *Islanded microgrid system including robust T-S and droop controller*

3 Fuzzy T-S system description of AC microgrid

It has been shown that T-S fuzzy models with linear rule consequences can approximate any smooth non-linear system [23]. This approach uses linear approximated subsystems to describe non-linearity of the system dynamics. They also offer a systematic procedure to design controllers and observers for non-linear systems such as the one in (6). T-S models are based on IF–THEN rules like other fuzzy inference systems, while each rule describes a region of the physical system's behavior.

The *i*th rule of the T-S fuzzy model is of the following form:

rule *i*: IF $z_1(t)$ is $M_{i1}(t)$ and … and $z_p(t)$ is $M_{ip}(t)$

$$\text{THEN} \begin{cases} \dot{x}(t) = A_i x(t) + B_i u(t) \\ y(t) = C_i x(t) \end{cases} \quad i = 1, 2, \ldots, r$$

where r is the number of total rule, $z_1(t)\ldots z_p(t)$ are the premise variables that can be function of state, disturbance and/or time. $M_{i1}(t), \ldots, M_{ip}(t)$ are the fuzzy sets which correspond to their premise variables. Final outputs of T-S inference system can be indicated by

$$\begin{aligned} \dot{x}(t) &= \frac{\sum_{i=1}^{r} w_i(z(t))\{A_i x(t) + B_i u(t)\}}{\sum_{i=1}^{r} w_i(z(t))} \\ &= \sum_{i=1}^{r} h_i(z(t))\{A_i x(t) + B_i u(t)\} \\ y(t) &= \frac{\sum_{i=1}^{r} w_i(z(t))\{C_i x(t) + D_i u(t)\}}{\sum_{i=1}^{r} w_i(z(t))} \\ &= \sum_{i=1}^{r} h_i(z(t))\{C_i x(t) + D_i u(t)\} \end{aligned} \tag{8}$$

where in such equations we have

$$\begin{aligned} z(t) &= \begin{bmatrix} z_1(t) & z_2(t) & \ldots & z_p(t) \end{bmatrix} \\ w_i(z(t)) &= \prod_{j=1}^{p} M_{ij}(z_j(t)), h_i(z(t)) = \frac{w_i(z(t))}{\sum_{i=1}^{r} w_i(z(t))} \end{aligned} \tag{9}$$

It is always possible to choose suitable premise variables and membership functions to attain a T-S model with desired accuracy [23]. To obtain fuzzy T-S system for our defined non-linear system (1), premise variables are considered as non-linear terms in (1) and they are given as follows:

$$z_1(t) \equiv \frac{p_{\mathrm{f}}}{v_d^2 + v_q^2}, \quad z_2(t) \equiv \frac{(s_b/v_b^2)q_{\mathrm{f}} - (\omega_{\mathrm{pu}}/z_b)x_{L_{\mathrm{pu}}}(i_d^2 + i_q^2)}{v_d^2 + v_q^2}. \tag{10}$$

System states i_d, i_q, v_d and v_q are inputs to the fuzzy system and for driving z_1 and z_2, they are required to be measured for each DGs. In our case, based on non-linear sector method, z_1 and z_2 are approximated by two membership function as follows:

$$\begin{aligned} z_1(t) &= M_1(z_1(t))(\overline{Z_1}) + M_2(z_1(t))(\underline{Z_1}) \\ z_2(t) &= N_1(z_2(t))(\overline{Z_2}) + N_2(z_2(t))(\underline{Z_2}) \end{aligned} \tag{11}$$

where $(\overline{Z_i})$ and $(\underline{Z_i})$ are upper and lower bound for premise variables, respectively. Also in this method, we should have

$$\begin{aligned} M_1(z_1(t)) + M_2(z_1(t)) &= 1 \\ N_1(z_2(t)) + N_2(z_2(t)) &= 1 \end{aligned} \tag{12}$$

From (11) and (12), the membership functions can be calculated as

$$\begin{aligned} M_1(z_1(t)) &= \frac{(z_1(t) - \underline{Z_1})}{(\overline{Z_1} - \underline{Z_1})} \quad M_2(z_1(t)) = 1 - M_1(z_1(t)) \\ N_1(z_2(t)) &= \frac{(z_2(t) - \underline{Z_2})}{(\overline{Z_2} - \underline{Z_2})} \quad N_2(z_2(t)) = 1 - N_1(z_2(t)) \end{aligned} \tag{13}$$

and finally, by using non-linear sector method, T-S model can be written as follows: (see (14)) where in these equations, $\boldsymbol{B}$ and $\boldsymbol{C}$ are constant matrices defined in (6), $\boldsymbol{A}_1$, $\boldsymbol{A}_2$, $\boldsymbol{A}_3$ and $\boldsymbol{A}_4$ are matrices calculated using non-linear sector method and the fuzzy sets in (13). An additive uncertainty with ($\Delta\boldsymbol{A}$, $\Delta\boldsymbol{B}$, $\Delta\boldsymbol{C}$) realisation is considered at (14). Since it is a common assumption that the model is quite accurate for low frequencies but deteriorates in the high-

$$\begin{aligned} &\text{Rule 1: IF } z_1 \text{ is } M_1(z_1) \text{ and } z_2 \text{ is } N_1(z_2) \text{ THEN } \dot{x} = \mathrm{diag}(\boldsymbol{A}_1, \Delta\boldsymbol{A})x + (\boldsymbol{B}, \Delta\boldsymbol{B})^T u \\ &\text{Rule 2: IF } z_1 \text{ is } M_1(z_1) \text{ and } z_2 \text{ is } N_2(z_2) \text{ THEN } \dot{x} = \mathrm{diag}(\boldsymbol{A}_2, \Delta\boldsymbol{A})x + (\boldsymbol{B}, \Delta\boldsymbol{B})^T u \\ &\text{Rule 3: IF } z_1 \text{ is } M_2(z_1) \text{ and } z_2 \text{ is } N_1(z_2) \text{ THEN } \dot{x} = \mathrm{diag}(\boldsymbol{A}_3, \Delta\boldsymbol{A})x + (\boldsymbol{B}, \Delta\boldsymbol{B})^T u \\ &\text{Rule 4: IF } z_1 \text{ is } M_2(z_1) \text{ and } z_2 \text{ is } N_2(z_2) \text{ THEN } \dot{x} = \mathrm{diag}(\boldsymbol{A}_2, \Delta\boldsymbol{A})x + (\boldsymbol{B}, \Delta\boldsymbol{B})^T u \\ &\text{Output for all fuzzy rules: } y = (\boldsymbol{C} \quad \Delta\boldsymbol{C})x \end{aligned} \tag{14}$$

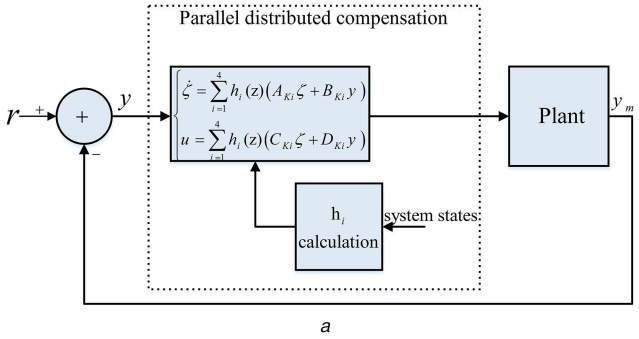

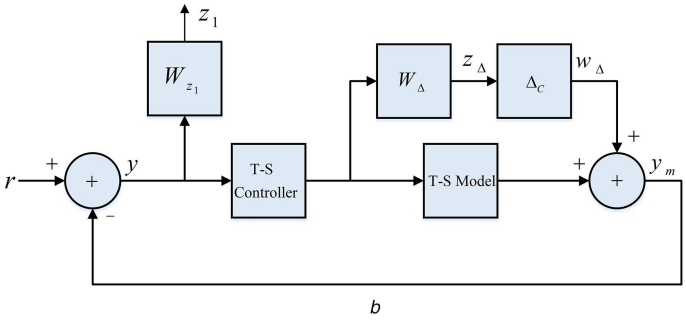

Fig. 4 *Controller details.*
(a) PDC structure in the closed-loop form, ***(b)*** Closed-loop extended model with weights

frequency range. The reason is that the effects of parasitics and non-linearities become more significant at higher frequencies.

Fig. 4*a* shows controller structure which is used in the design procedures. This controller comprises several locally linear controllers and the whole control system is known as parallel distributed compensator (PDC).

Although, linear dynamic robust controller can be designed for each subsystem separately, but such an approach does not guarantee robust performance or even stability of the whole system. Therefore, in the next section, a unified control system design is proposed which is based on just one optimisation problem instead of dealing with four separate cases.

4 Robust H_∞ controller design for T-S model

H_∞ controller can handle uncertainties and external disturbances in the defined model (6) appropriately. Unfortunately, its designing method is not straightforward at all because solving Hamilton Jacobi Isaacs partial differential equation is required, by a closed form solution, to drive non-linear robust controller. Therefore, T-S fuzzy system provides us a systematic paradigm for designing locally linear H_∞ controller. H_∞ linear controller design is a well-established method in control system theory where its design procedure is generally accomplished by using LMIs [24, 25]. The conventional design procedure can be extended to T-S models with some appropriate assumptions. The additive unstructured uncertainty Δ which represents unmodelled and high-frequency dynamics is considered in design procedures as follows:

$$\begin{aligned} &\| \Delta \|_\infty \le \gamma \\ &G = G_i + \Delta = G_i + W_D \Delta_c \\ &\Delta_c := \left\{ \Delta_c \in \mathbb{C}^{2\times 2} \middle| \ \| \Delta_c \|_\infty \le 1 \right\} \\ &\Delta_c = \begin{pmatrix} \Delta_{11} & \Delta_{12} \\ \Delta_{21} & \Delta_{22} \end{pmatrix} W_D \le \gamma \end{aligned} \tag{15}$$

where G_i is the nominal transfer function for each subsystem (A_i, B, C), W_Δ indicates upper bounds and frequency behavior of uncertainty and Δ_c represents lumped uncertainty.

(see (16)) .

Fig. 4*b* shows virtual closed-loop diagram with appropriate weighting functions that represent design objectives in this problem which are listed as follow:

(i) $\| T_{W_\Delta Z_\Delta} \|_\infty < 1$ Robust Stability
(ii) $\| T_{rZ_1} \|_\infty < 1$ Nominal Performance

where $T_{(W_\Delta Z_\Delta)}$ and $T_{(rZ_1)}$ are the transfer functions from w_Δ and r to z_Δ and z_1, respectively. It can be shown that the first two objectives can be achieved by a vector norm inequality as follows [26]:

$$\left\| \begin{matrix} T_{W_\Delta Z_\Delta} \\ T_{rZ_1} \end{matrix} \right\|_\infty < 1 \tag{17}$$

We need to construct the linear fractional transformation equation to solve (17). By defining $z = \begin{pmatrix} z_\Delta \\ z_1 \end{pmatrix}$ and $w = \begin{pmatrix} w_\Delta \\ r \end{pmatrix}$, open-loop interconnected (18) can be written using the derived T-S model and weighting function state-space realisation as follows:

$$P: \begin{cases} \dot{\tilde{x}} = \left(\sum_{i=1}^{4} (h_i(z)\tilde{A}_i)\tilde{x} \right) + B_w w + B_u u \\ z = C_z \tilde{x} + D_{zw} w + D_z u \\ y = C_y \tilde{x} + D_w w \end{cases} \tag{18}$$

where $\tilde{x} = \left(x, x_{W_\Delta}, x_{W_{z_1}}\right)^{\mathrm{T}}$ and P follow the same T-S fuzzy inference system as described in (8)–(14). Consider the following T-S controller K as

$$K: \begin{cases} \dot{\zeta} = \sum_{i=1}^{4} h_i(z)(A_{Ki}\zeta + B_{Ki} y) \\ u = \sum_{i=1}^{4} h_i(z)(C_{Ki}\zeta + D_{Ki} y) \end{cases} \tag{19}$$

By applying controller (19) to (18) the closed-loop system is obtained as

$$\begin{aligned} &\min \gamma \\ &\text{such that} \\ &\begin{pmatrix} \tilde{A}_i X + X\tilde{A}_i^{\mathrm{T}} + B_u \hat{C}_i + \left(B_u \hat{C}_i\right)^{\mathrm{T}} & * & * & * \\ \hat{A}_i + \left(\tilde{A}_i + B_u \hat{D}_i C_y\right)^{\mathrm{T}} & \tilde{A}_i^T Y + Y\tilde{A}_i + \hat{B}_i C_y + \left(\hat{B}_i C_y\right)^{\mathrm{T}} & * & * \\ \left(B_w + B_u \hat{D}_i D_w\right)^{\mathrm{T}} & \left(YB_w + \hat{B}_i D_w\right)^{\mathrm{T}} & -\gamma I & * \\ C_z X + D_z \hat{C}_i & C_Z + D_Z \hat{D}_i C_y & D_{zw} + D_z \hat{D}_i D_w & -\gamma I \end{pmatrix} < 0 \quad i = 1, 2, 3, 4. \\ &\begin{pmatrix} X & I \\ I & Y \end{pmatrix} > 0 \end{aligned} \tag{16}$$

$$T:\begin{cases} x_{cl} = \sum_{i=1}^{4} h_i(z)\left(\bar{A}_i x_{cl} + \bar{B}_i w\right) \\ z = \sum_{i=1}^{4} h_i(z)\left(\bar{C}_i x_{cl} + \bar{D}_i w\right) \end{cases} \tag{20}$$

where

$$\bar{A}_i = \begin{pmatrix} \tilde{A}_i + B_u D_{Ki} C_y & B_u C_{Ki} \\ B_{Ki} C_y & A_{Ki} \end{pmatrix}, \quad \bar{B}_i = \begin{pmatrix} B_w B_u D_{Ki} D_w \\ B_{Ki} D_w \end{pmatrix}$$
$$\bar{C}_i = \begin{pmatrix} C_z + D_z D_{ki} C_y & D_z C_{Ki} \end{pmatrix}, \quad \bar{D}_i = (D_{zw} + D_z D_{Ki} D_w) \tag{21}$$

It should be noted that the whole closed-loop system uses inference engine given by (14). It can be shown that the closed-loop system (20) has L_2 gain less than $\gamma > 0$ if there exist a matrix $\boldsymbol{P} > 0$ such that [27]

$$\begin{pmatrix} \boldsymbol{P}\bar{A}_i + \boldsymbol{P}\bar{A}_i^{\mathrm{T}} & \boldsymbol{P}\bar{B}_i & \bar{C}_i^{\mathrm{T}} \\ \bar{B}_i^{\mathrm{T}} P & -\gamma I & \bar{D}_i^{\mathrm{T}} \\ \bar{C}_i & \bar{D}_i & -\gamma I \end{pmatrix} < 0 \quad i = 1, 2, 3, 4 \tag{22}$$

It can be derived that (22) is the sufficient condition for having L_2 gain performance which is known as the H_∞ criterion.

However, controller K cannot be calculated using (22), since it is not a convex problem. By defining $\boldsymbol{P} = \begin{pmatrix} Y & N \\ N^T & * \end{pmatrix}$, $\boldsymbol{P}^{-1} = \begin{pmatrix} X & M \\ M^T & * \end{pmatrix}$ and also introducing a new set of variables as

$$\begin{cases} \hat{A}_i := NA_{Ki}M^T + NB_{Ki}C_yX + YB_uC_{Ki}M^T \\ \quad + Y\left(\tilde{A}_i + B_uD_{Ki}C_y\right)X \\ \hat{B}_i := NB_{Ki} + YB_uD_{Ki} \qquad i = 1, 2, 3, 4 \\ \hat{C}_i := C_{Ki}M^T + D_{Ki}C_yX \\ \hat{D}_i := D_{Ki} \end{cases} \tag{23}$$

non-convex offline optimisation (22) is converted to an LMI-based offline convex optimisation problem. It is shown that H_∞ problem (22) admits a solution, if there exists $X > 0$, $Y > 0$ and $\hat{A}_i, \hat{B}_i, \hat{C}_i, \hat{D}_i$ such that LMI formulation (16) is satisfied (see bottom of the page 5). Controller parameters $A_{Ki}, B_{Ki}, C_{Ki}, D_{Ki}$ are given by

$$\begin{cases} D_{Ki} = \hat{D}_i \\ C_{Ki} = \left(\hat{C}_i - D_{Ki}C_yX\right)\boldsymbol{M}^{-T} \\ B_{Ki} = \boldsymbol{N}^{-1}\left(\hat{B}_i - YB_uD_{Ki}\right) \qquad i = 1, 2, 3, 4 \\ A_{Ki} = \boldsymbol{N}^{-1}\left(\hat{A}_i - NB_{Ki}C_yX - YB_uC_{Ki}\boldsymbol{M}^T\right) \\ \quad - Y\left(\tilde{A}_i + B_uD_{Ki}C_y\right)X)\boldsymbol{M}^{-T}) \end{cases} \tag{24}$$

where $\boldsymbol{M}$ and $\boldsymbol{N}$ are non-singular matrices satisfy the following equation:

$$YX + \boldsymbol{N}\boldsymbol{M}^T = I\,. \tag{25}$$

In this problem, desired closed-loop response characteristics such as system bandwidth and steady-state error, W_{z_1} is selected as performance weighting function. The performance weighting function (W_{z_1}) should be similar to step function since steady-state values for V_d and V_q have DC forms. Precise location of the poles and zeros are degrees of freedom which can be used to achieve better performance by controller designer. In our design W_{z_1} is considered as

$$W_{z_1} = \begin{pmatrix} \dfrac{s+50}{s+0.02} & 0 \\ 0 & \dfrac{s+50}{s+0.02} \end{pmatrix} \tag{26}$$

Moreover, W_Δ is chosen as robust stability weighting function for having suitable sensitivity function and as an upper bound for uncertainty Δ. W_Δ should be considered as a stable transfer function with maximum singular value placed at frequencies higher than AC microgrid nominal frequency. Thus, W_Δ is considered as follows:

$$W_\Delta = \begin{pmatrix} \dfrac{s+0.9}{s+1.1} & 0 \\ 0 & \dfrac{s+0.9}{s+1.1} \end{pmatrix} \tag{27}$$

Designed controller matrices are given in Appendix. Both DGs in studied microgrid uses same controllers although they have different power ratings.

5 Simulation results

In this section, the performance of the proposed T-S robust controller for the studied AC microgrid in Fig. 3 is investigated under different scenarios. Microgrid system parameter and interval for fuzzy variables are given in Table 1. When premise variable bounds have been set, considering permissible values for the system states (1), regardless of their values, desirable performance of the T-S robust controller can be achieved by appropriate choosing of weighting function (26).

The system is simulated by MATLAB/SimPowerSystem toolbox. Specifically, robust stability and nominal performance of the microgrid system with respect to the linear and non-linear load dynamics and accidental outage of a DG are studied. Moreover, the performance of the T-S robust controller is compared with conventional cascaded PI controllers at defined load dynamics for T-S robust controller performance test.

5.1 Performance with linear load

In this case study, at $t = 0.5$ s a 3 kVA linear load with PF = 0.85 is connected to the microgrid. When system states reached to stable condition, at $t = 0.8$ s a 1.5 kVA linear load with PF = 0.85 is subtracted from the PCC PCC main load. Fig. 5*a* shows *d*–*q* components of PCC voltage. As it can be seen from the figure, T-S controller can damp oscillations caused by load increase and decrease, appropriately. Figs. 5*b* and *c* show active and reactive power, respectively. As these figures indicate active and reactive power of the linear load is shared between DGs according to their

Table 1 Parameters of the microgrid system

Quantity	Value
S_{base}, S_1, S_2	10, 5, 10 kVA
L_f (series inductance)	5 mH
C_f (shunt capacitance)	470 μF
f_{sw} (PWM carrier frequency)	6 kHz
droop parameters of DG1	$m_1 = 0.006, n_1 = 1.5$
droop parameters of DG2	$m_2 = 0.002, n_2 = 1$
V_{ac} (microgrid phase voltage)	220
f_0 (system frequency)	50 Hz
V_{dc} (DC bus voltage)	600 V
Z_{line1}	0.018 + j0.039
Z_{line2}	0.015 + j0.034
LPF time constant	1 ms
$\overline{Z_1}, \underline{Z_1}$	−0.1, 0.3
$\overline{Z_2}, \underline{Z_2}$	−0.2, 0.1

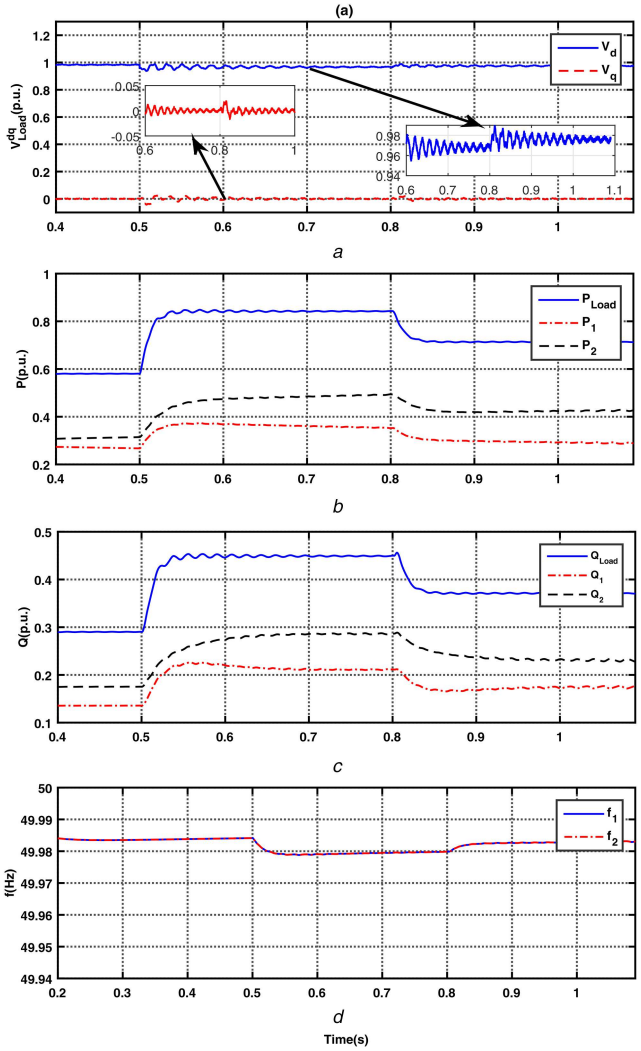

Fig. 5 *Imposition and reduction of linear load at t = 0.5 s and t = 0.8 s:*
(a) *dq* components of PCC voltage, ***(b)*** real power of DG units and load, ***(c)*** reactive power of DG units and load, ***(d)*** DGs droop frequencies

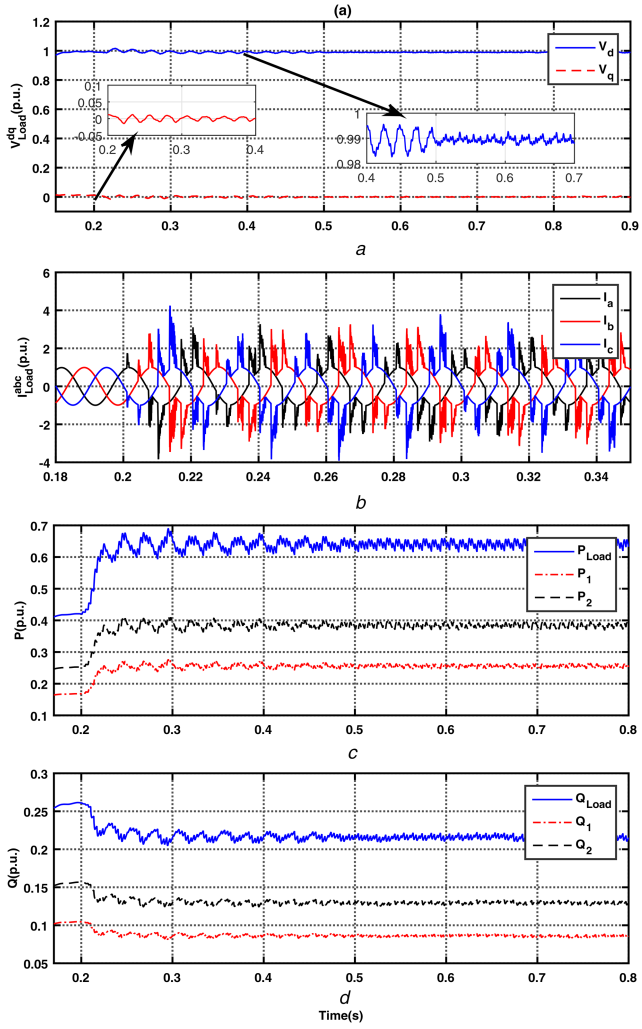

Fig. 6 *Imposition of non-linear load at t = 0.2 s:*
(a) *dq* components of PCC voltage, ***(b)*** 3-ph instantaneous load currents, ***(c)*** real power of DG units and load, ***(d)*** reactive power of DG units and load

droop coefficients. Fig. 5*d* shows frequency profile of each DG changed according to their droop coefficients. Therefore, robust T-S controller shows satisfying performance in the presence of imposition and reduction of linear load.

5.2 Performance with non-linear load

Power electronic converters with regulated output power have response characteristic as CPL with negative impedance effect (e.g. motor drive with regulated speed) [28]. To show the robustness of the proposed controller structure with such loads, a 3−ph rectifier connected to a buck converter while supplying a 2 kW CPL, is imposed to the AC bus while microgrid is supplying a 5 kVA linear load with PF = 0.9 and required power is provided by DGs according to their droop coefficients.

d–*q* components of PCC voltage are depicted in Fig. 6*a*. As it can be seen from this figure except for a short-time transient, T-S controller successfully regulates PCC voltage. Fig. 6*b* shows 3−ph instantaneous load current which has harmonic due to highly non-linear load. Figs. 6*c* and *d* show active and reactive power increase are shared appropriately between DGs. Consequently, robust T-S controller could maintain system stability in the presence of CPL.

5.3 Accidental DG outage

The objective of this case study is to show that robust T-S controller can maintain microgrid voltage and frequency stability after a sudden accidental outage of DG1. This scenario can happen when a DG should be overhauled, or in the case of primary energy source disturbances.

At $t = 0.4$ s, while microgrid is supplying a 5 kVA linear load with PF = 0.85 at its PCC, DG1 breaker is opened. Figs. 7*a* and *b* show that after a very short transient, PCC voltage is regulated at droop reference outputs. Figs. 7*c* and *d* show active and reactive power of DGs and load. As depicted in these figures, T-S controller robustly regulates voltage and current such that deficit power in the microgrid is compensated by DG2.

5.4 Comparison with conventional PI controller

PI controller is one of the first options for microgrid control problems because of its simple intuitive design and relative robustness against external disturbances [29, 30]. However, using linearised equation for system model around operating point can degrade system performance in case of changes in load dynamic and configuration of the system. In this section, inner current and outer voltage loop PI controllers are used instead of T-S robust controller to show the effectiveness of the T-S controller. PI controllers are designed such that (1) have appropriate gain and phase margin for each input and output channels. PI controller parameters are given in Table 2.

Simulation conditions in these scenarios are similar to T-S robust controller cases so results can be compared conveniently.The obtained results of V_d and V_q have been included in two separate Figs. 8 and 9 to improve comparability of robust T-S fuzzy controller with the conventional PI controller. Figs. 8 and 9 depict in almost all scenarios robust T-S controller yield better performance with respect to settling time and oscillation than the conventional PI controller for both V_d and V_q components of PCC voltage. Moreover, it can be seen from Figs. 8 and 9*b*, *c* that the

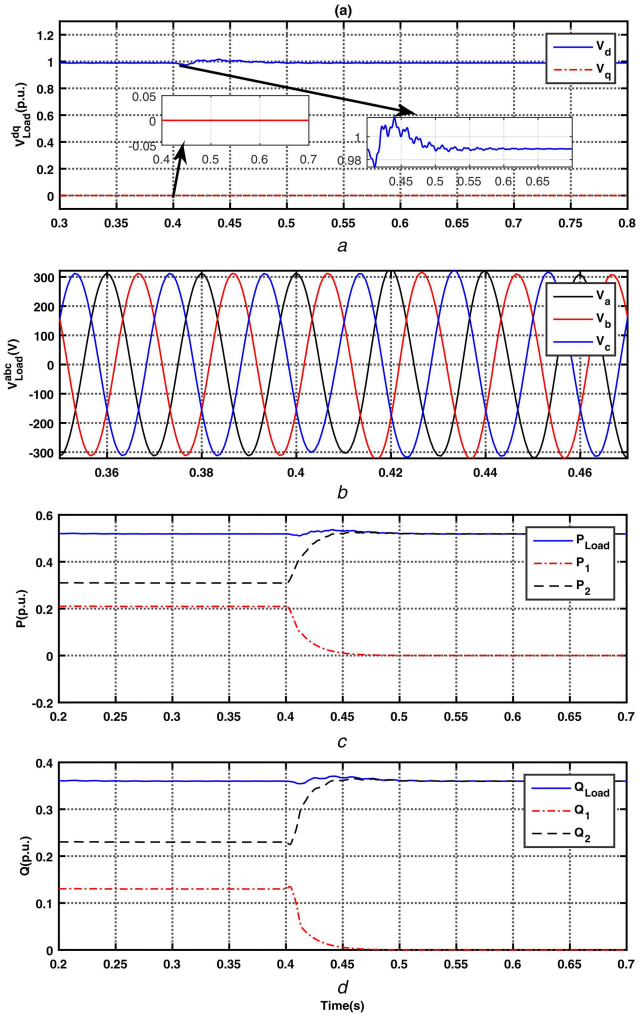

Fig. 7 *DG1 accidental outage at t = 0.4 s:*
(a) *dq* components of PCC voltage, ***(b)*** PCC instantaneous voltages, ***(c)*** real power of DG units and load, ***(d)*** reactive power of DG units and load

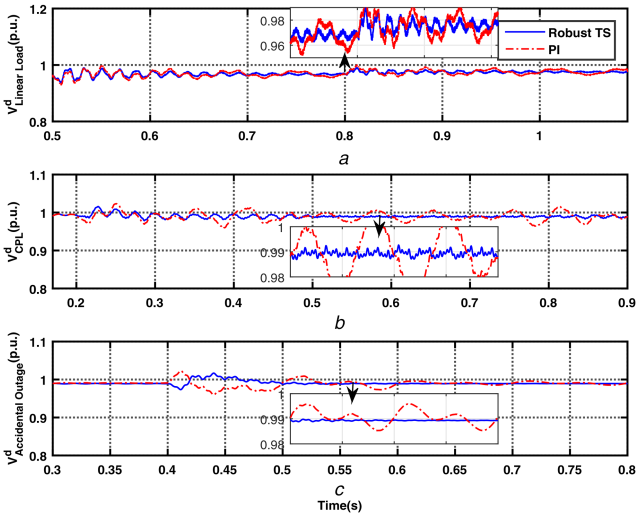

Fig. 8 *V_d component of PCC voltage for robust T-S and cascaded PI controllers for defined load dynamic:*
(a) Linear Load, ***(b)*** Constant power load, ***(c)*** Accidental outage

controller performance has been deteriorated drastically in CPL and accidental outage of DG1 cases. In these two scenarios, V_d and V_q response oscillate around the references provided by droop controller and PI controller is unable to diminish these oscillations. As a result, complexity of the T-S robust controller is justified by its better performance in different load dynamics and disturbances for the system.

Table 2 Cascaded PI controller parameters

Output channel	Current controller	Voltage controller
V_d	$k_p = 10, k_i = 500$	$k_p = 0.5, k_i = 10$
V_q	$k_p = 25, k_i = 600$	$k_p = 0.1, k_i = 15$

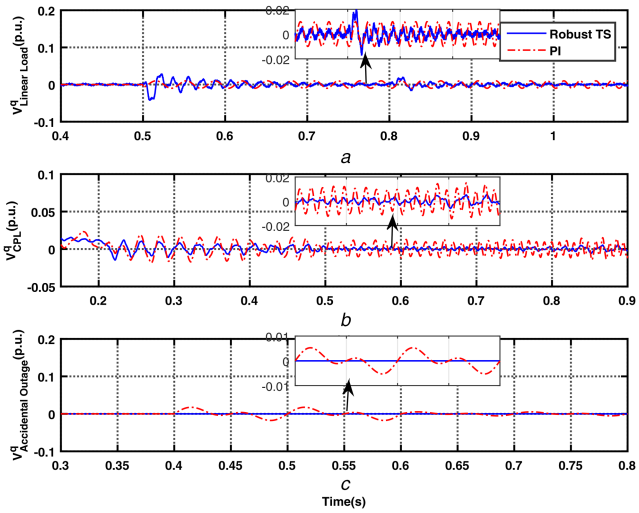

Fig. 9 *V_d component of PCC voltage for robust T-S and cascaded PI controllers for defined load dynamic:*
(a) Linear load, ***(b)*** Constant power load, ***(c)*** Accidental outage

6 Conclusion

A fuzzy decentralised robust control strategy for the autonomous operation of an islanded AC microgrid to regulate voltage and frequency was proposed in this paper. A dual locally linear model for the non-linear state-space equation in *d–q* frame using T-S fuzzy interference engine is derived. Sufficient conditions for guaranteeing robust stability and L_2 gain performance (H_∞ criterion) are expressed using an extension of Bounded Real Lemma. Design objective is formulated as a non-convex optimisation problem reduced to a convex LMI problem which is solvable in finite time using MATLAB LMI toolbox. Design procedure can be extended to other microgrid topologies very conveniently by defining new premise variables and design objectives. The proposed controller shows very good performance characteristics in various scenarios with different load dynamics (linear and non-linear) and DG accidental outage. Moreover, simulation results for cascaded PI controllers confirm the superiority of T-S robust controller in the non-linear load condition and accidental outage of DGs.

7 Acknowledgments

This work was supported by the Institute for Research in Fundamental Sciences (IPM) under Grant CS 1397-4-56.

8 References

[1] Hatziargyriou, N., Asano, H., Iravani, R., *et al.*: 'Microgrids', *IEEE Power Energy Mag.*, 2007, **5**, (4), pp. 78–94
[2] Lasseter, R. H., Paigi, P.: 'Microgrid: a conceptual solution': 2004 IEEE 35th Annual Power Electronics Specialists Conf. (IEEE Cat. No.04CH37551), Aachen, Germany, June 2004, **6**, pp. 4285–4290
[3] Han, H., Hou, X., Yang, J., *et al.*: 'Review of power sharing control strategies for islanding operation of ac microgrids', *IEEE Trans. Smart Grid*, 2016, **7**, (1), pp. 200–215
[4] Guerrero, J. M., Vasquez, J. C., Matas, J., *et al.*: 'Hierarchical control of droop-controlled ac and dc microgrids; a general approach toward standardization', *IEEE Trans. Ind. Electron.*, 2011, **58**, (1), pp. 158–172
[5] Etemadi, A. H., Davison, E. J., Iravani, R.: 'A generalized decentralized robust control of islanded microgrids', *IEEE Trans. Power Syst.*, 2014, **29**, (6), pp. 3102–3113

[6] Babazadeh, M., Karimi, H.: 'A robust two-degree-of-freedom control strategy for an islanded microgrid', *IEEE Trans. Power Deliv.*, 2013, **28**, (3), pp. 1339–1347
[7] Karimi, H., Yazdani, A., Iravani, R.: 'Robust control of an autonomous four-wire electronically-coupled distributed generation unit', *IEEE Trans. Power Deliv.*, 2011, **26**, (1), pp. 455–466
[8] Tan, K. T., So, P. L., Chu, Y. C., *et al.*: 'Coordinated control and energy management of distributed generation inverters in a microgrid', *IEEE Trans. Power Deliv.*, 2013, **28**, (2), pp. 704–713
[9] Isidori, A.: '*Nonlinear control systems: an introduction*' (Springer-Verlag, New York, NY, USA, 1985, 3rd edn.), pp. 120–140
[10] Mahmud, M. A., Hossain, M. J., Pota, H. R., *et al.*: 'Robust nonlinear distributed controller design for active and reactive power sharing in islanded microgrids', *IEEE Trans. Energy Convers.*, 2014, **29**, (4), pp. 893–903
[11] Cucuzzella, M., Incremona, G. P., Ferrara, A.: 'Design of robust higher order sliding mode control for microgrids', *IEEE J. Emerg. Sel. Top. Circuits Syst.*, 2015, **5**, (3), pp. 393–401
[12] Wai, R. J., Lin, C. Y., Wu, W. C., *et al.*: 'Design of backstepping control for high-performance inverter with stand-alone and grid-connected power-supply modes', *IET Power Electron.*, 2013, **6**, (4), pp. 752–762
[13] Mahmud, M. A., Hossain, M. J., Pota, H. R., *et al.*: 'Robust nonlinear controller design for three-phase grid-connected photovoltaic systems under structured uncertainties', *IEEE Trans. Power Deliv.*, 2014, **29**, (3), pp. 1221–1230
[14] Valencia, F., Collado, J., Sáez, D., *et al.*: 'Robust energy management system for a microgrid based on a fuzzy prediction interval model', *IEEE Trans. Smart Grid*, 2016, **7**, (3), pp. 1486–1494
[15] Sekhar, P. C., Mishra, S., Sharma, R.: 'Data analytics based neuro-fuzzy controller for diesel-photovoltaic hybrid ac microgrid', *IET Gener., Transm. Distrib.*, 2015, **9**, (2), pp. 193–207
[16] Sefa, I., Altin, N., Ozdemir, S., *et al.*: 'Fuzzy pi controlled inverter for grid interactive renewable energy systems', *IET Renew. Power Gener.*, 2015, **9**, (7), pp. 729–738
[17] Hasanien, H. M., Matar, M.: 'A fuzzy logic controller for autonomous operation of a voltage source converter-based distributed generation system', *IEEE Trans. Smart Grid*, 2015, **6**, (1), pp. 158–165
[18] Bevrani, H., Habibi, F., Babahajyani, P., *et al.*: 'Intelligent frequency control in an ac microgrid: online PSO-based fuzzy tuning approach', *IEEE Trans. Smart Grid*, 2012, **3**, (4), pp. 1935–1944
[19] Sáez, D.,, Ávila, F., Olivares, D., *et al.*: 'Fuzzy prediction interval models for forecasting renewable resources and loads in microgrids', *IEEE Trans. Smart Grid*, 2015, **6**, (2), pp. 548–556
[20] Kakigano, H., Miura, Y., Ise, T.: 'Distribution voltage control for dc microgrids using fuzzy control and gain-scheduling technique', *IEEE Trans. Power Electron.*, 2013, **28**, (5), pp. 2246–2258
[21] Kim, D. E., Lee, D. C.: 'Feedback linearization control of three-phase ups inverter systems', *IEEE Trans. Ind. Electron.*, 2010, **57**, (3), pp. 963–968
[22] Rigatos, G., Siano, P., Zervos, N., *et al.*: 'Decentralised control of parallel inverters connected to microgrid using the derivative-free non-linear Kalman filter', *IET Power Electron.*, 2015, **8**, (7), pp. 1164–1180
[23] Tanaka, K., Wang, H. O.: '*Fuzzy control systems design and analysis: a LMI approach*' (Wiley, New York, NY, USA, 2001), pp. 277–289
[24] Boyd, S., Ghaoui, L. E., Feron, E., *et al.*: '*Linear matrix inequalities in systems and control theory*' (SIAM, Philadelphia, PA, USA, 1994)
[25] Scherer, C., Gahinet, P., Chilali, M.: 'Multiobjective output-feedback control via LMI optimization', *IEEE Trans. Autom. Control*, 1997, **42**, (7), pp. 896–911
[26] Zhou, K., Doyle, J. C.: '*Essentials of robust control*' (Prentice Hall, Upper Saddle River, NJ, USA, 1997), pp. 81–100
[27] Xie, W.: 'Improved l2 gain performance controller synthesis for Takagi-Sugeno fuzzy system', *IEEE Trans. Fuzzy Syst.*, 2008, **16**, (5), pp. 1142–1150
[28] Emadi, A., Khaligh, A., Rivetta, C. H., *et al.*: 'Constant power loads and negative impedance instability in automotive systems: definition, modeling, stability, and control of power electronic converters and motor drives', *IEEE Trans. Veh. Technol.*, 2006, **55**, (4), pp. 1112–1125
[29] Mohamed, Y. A. R. I., El-Saadany, E. F.: 'Adaptive decentralized droop controller to preserve power sharing stability of paralleled inverters in distributed generation microgrids', *IEEE Trans. Power Electron.*, 2008, **23**, (6), pp. 2806–2816
[30] Bidram, A., Davoudi, A., Lewis, F. L., *et al.*: 'Secondary control of microgrids based on distributed cooperative control of multi-agent systems', *IET Gener., Transm. Distrib.*, 2013, **7**, (8), pp. 822–831

9 Appendix

Matrices of controller used in simulation section are as follows: (see equation below) (see equation below) (see equation below) (see equation below)

$$A_{K1} = \begin{pmatrix} -1.8 & -625.0 & -600.5 & -465.0 & 105.7 & 362.1e^{-3} \\ -33.6 & -15.9e^{3} & -20.8e^{3} & -10.7e^{3} & 2.3e^{3} & -26.2 \\ -138.8 & 6.2e^{3} & -23.5e^{3} & -14.0e^{3} & -3.5e^{3} & 930.3 \\ -81.7 & 3.1e^{3} & -12.5e^{3} & -8.4e^{3} & -1.8e^{3} & 531.8 \\ -4.4 & 4.5e^{3} & 3.0e^{3} & 1.3e^{3} & -911.5 & 91.2 \\ 1.1 & -84.8 & -84.8 & -24.8 & 75.5 & -11.1 \end{pmatrix}$$

$$B_{K1} = \begin{pmatrix} -6.86 & 295.71e^{-3} \\ 1.13 & 18.50 \\ 548.86e^{-3} & 72.09 \\ 7.58 & 39.03 \\ 144.42e^{-3} & 4.47 \\ 1.27 & -484.05e^{-3} \end{pmatrix} \quad D_{K1} = \begin{pmatrix} 40.73e^{-3} & -2.62e^{-3} \\ -4.47e^{-3} & 1.83e^{-3} \end{pmatrix}$$

$$C_{K1} = \begin{pmatrix} -5.19 & 1.29 & 6.30 & -8.24 & -358.06e^{-3} & -69.71e^{-3} \\ -247.71e^{-3} & 82.25 & 69.09 & 35.28 & -13.29 & 1.08 \end{pmatrix}$$

$$A_{K2} = \begin{pmatrix} -16.6e^3 & -7.2e^3 & -2.6e^3 & 151.0 & -4.0e^3 & -165.8 \\ -6.1e^3 & -3.3e^3 & 2.3e^3 & 77.6 & -2.3e^3 & -126.3 \\ -23.4e^3 & -7.6e^3 & -25.0e^3 & 374.2 & 43.1 & 1.6e^3 \\ 291.9 & -139.9 & 334.7 & -59.8 & 67.7 & -244.5 \\ 1.5e^3 & 16.2 & 4.9e^3 & -67.3 & -883.3 & -467.0 \\ 1.3e^3 & -843.3 & 1.9e^3 & -149.3 & 247.0 & -595.4 \end{pmatrix}$$

$$B_{K2} = \begin{pmatrix} 7.44 & -51.02 \\ -2.76 & -24.46 \\ 3.81 & -42.80 \\ 13.34 & 184.22e^{-3} \\ 2.38 & -4.27 \\ 782.88e^{-3} & 1.40 \end{pmatrix} \quad D_{K2} = \begin{pmatrix} 17.89e^{-3} & -8.61e^{-3} \\ 5.60e^{-3} & -2.31e^{-3} \end{pmatrix}$$

$$C_{K2} = \begin{pmatrix} -6.51 & -398.10e^{-3} & -11.13 & 2.27 & 654.65e^{-3} & -2.59 \\ -42.66 & -4.13 & -95.87 & 2.23 & 10.88 & 10.93 \end{pmatrix}$$

$$A_{K3} = \begin{pmatrix} -803.4 & -482.1e^3 & -131.1 & -1.3e^3 & -21.5e^3 & 2.2e^3 \\ -331.3 & -206.0e^3 & -59.8 & -1.3e^3 & -17.0e^3 & -492.5 \\ 34.4 & 12.5e^3 & -800.2 & -850.1 & -8.6 & -1.6e^3 \\ -399.7 & -228.2 & -76.5 & -565.2e^{-3} & 65.1 & -34.1 \\ 10.4 & 5.4e^3 & 926.3 & -83.3 & -279.6 & -494.0 \\ 5.5 & 3.2e^3 & 36.3 & 52.8 & 2.4e^3 & -1.0e^3 \end{pmatrix}$$

$$B_{K3} = \begin{pmatrix} -4.12 & 1.21e^3 \\ 556.62e^{-3} & 668.96 \\ 4.28 & 82.68 \\ 111.09 & 608.14e^{-3} \\ -13.27 & -6.90 \\ -20.25 & -4.60 \end{pmatrix} \quad D_{K3} = \begin{pmatrix} 44.41e^{-3} & -22.87e^{-3} \\ 5.87e^{-3} & -1.23e^{-3} \end{pmatrix}$$

$$C_{K3} = \begin{pmatrix} 22.72 & 12.72 & 2.64 & 801.82e^{-3} & 543.05e^{-3} & 3.30 \\ 1.16e^3 & 603.94 & 113.66 & -8.46 & -68.23 & -26.46 \end{pmatrix}$$

$$A_{K4} = \begin{pmatrix} -473.3 & -1.0e^3 & -40.6e^3 & -30.9e^3 & -1.1e^3 & -248.3 \\ 1.6e^3 & 9.5 & 43.4e^3 & 33.1e^3 & 1.5e^3 & 115.9 \\ 80.9e^3 & -107.5e^3 & -639.1e^3 & -486.6e^3 & -3.9e^3 & -143.7 \\ 61.6e^3 & -81.9e^3 & -487.5e^3 & -371.1e^3 & -3.0e^3 & -111.8 \\ -991.7 & 1.8e^3 & 18.7e^3 & 14.2e^3 & 541.9 & -259.5 \\ -1.0e^3 & 6.1e^3 & 55.9e^3 & 42.8e^3 & 5.7e^3 & -1.8e^3 \end{pmatrix}$$

$$B_{K4} = \begin{pmatrix} 8.08 & 259.89 \\ 11.21 & 64.72 \\ -261.12 & -1.13e^3 \\ 425.81 & -860.58 \\ 9.33 & -108.74 \\ 27.80 & 51.01 \end{pmatrix} \quad D_{K4} = \begin{pmatrix} 3.42e^{-3} & -8.77e^{-3} \\ 4.97e^{-3} & -10.93e^{-3} \end{pmatrix}$$

$$C_{K4} = \begin{pmatrix} 5.00 & -693.63e^{-3} & 6.04 & 5.05 & 7.43 & -3.16 \\ 55.46 & -96.39 & -993.94 & -757.50 & -19.32 & -674.18e^{-3} \end{pmatrix}$$